Regional Studies in Marine Science 17 (2018) 17–27

Contents lists available at ScienceDirect

Regional Studies in Marine Science

journal homepage: www.elsevier.com/locate/rsma

Tidal and seasonal variation in carbonate chemistry, pH and salinity for a mineral-acidified tropical estuarine system

Sorya Proum [a,b], Jose H. Santos [c], Lee Hoon Lim [c], David J. Marshall [a,*]

[a] Environmental and Life Sciences, Faculty of Science, Universiti Brunei Darussalam, BE 1410 Jalan Tungku Link, Brunei Darussalam
[b] Chemistry Department, Royal University of Phnom Penh, Russian Federation Boulevard, Toul Kork, Phnom Penh, Cambodia
[c] Chemical Sciences, Universiti Brunei Darussalam, BE 1410 Jalan Tungku Link, Brunei Darussalam

HIGHLIGHTS

- Tidal fluxes and seasonal patterns in pH, salinity and carbonate chemistry are described for a tropical Southeast Asian estuary influenced by Acid Sulphate Soil (ASS) discharge.
- Heavy daily downpours had little effect on the water salinity and pH, whereas accumulative rainfall during the monsoon lowered these parameter's baselines.
- Remarkably low pH relative to salinity, extraordinary pCO_2 super-saturation, and carbonate under-saturation occurred extensively across the estuary.
- Mineral acidification is implicated in changing estuarine pH and elevating pCO_2 through the carbonate equilibrium system.

ARTICLE INFO

Article history:
Received 3 June 2017
Received in revised form 26 October 2017
Accepted 10 November 2017
Available online 21 November 2017

Keywords:
Acidification
Acid sulphate soil
Carbonate chemistry
Flooding
Tropical estuary
Southeast Asia

ABSTRACT

Estuarine acidification and carbonate chemistry derive from multiple biogeochemical processes. Other than biogenic CO_2-acidification, estuaries can be acidified allochthonously through non-carbonate sources originating in freshwater and land ecosystems. The present study considered the carbonate chemistry of a nutrified, turbid, tropical mangrove estuary, influenced by acidic groundwater discharge from pyritic soils (Acid Sulphate Soils, ASS). We studied the spatial and temporal variation of the surface water pH, salinity, total alkalinity (TA), partial pressure carbon dioxide (pCO_2), dissolved inorganic carbon (DIC), and calcite (Ω_{cal}) and aragonite (Ω_{ara}) saturation, in the Brunei Estuarine System (BES), Borneo, Southeast Asia. pH and salinity for tidal to seasonal timeframes were determined from data collected half-hourly, logged at three stations (upper, middle and lower estuary); these data were correlated with rainfall incidence and intensity. Carbonate parameters were calculated from TA using discrete samples collected from six stations. pH (6.8–7.9) and salinity (4.2–28.2) increased expectedly seawards, due to tidal forcing and freshwater dilution at opposite ends of the estuary; amplitudes within a tidal cycle became expanded landwards and during spring tides. While, the overall effect of heavy daily downpours on estuarine salinity and pH was muted, cumulative rainfall during the monsoon season distinctly lowered parameter baselines; the response was again more pronounced in the upper estuary. In the mid-to-upper estuary, we observed a remarkably low pH relative to salinity, extraordinary pCO_2 super-saturation (13031 ± 4412 μatm) and carbonate undersaturation (Ω_{cal} and Ω_{ara} were 0.006–1.431 and 0.004–0.928, respectively). Although the relative contributions of heterotrophic metabolism and ASS-discharge to the estuarine pH and pCO_2 were not determined, both processes are implicated in increasing both acidity and CO_2 levels. This study contributes to the understanding of carbonate fluxes in mineral-acidified estuaries.

1. Introduction

Estuarine carbonate systems are highly variable, both temporally (relative to tides and freshwater discharge) and spatially (within estuaries, locally and regionally). Understanding this variability is important to ecological frameworks (ecological structure and functioning), as well as marine, oceanic and atmospheric CO_2 flux contexts. Interest in marine carbonate systems has peaked against the backdrop of anthropogenic atmospheric CO_2 elevation (Noriega and Araujo, 2014); CO_2 in the atmosphere is rising at ~2 ppm per year (IPCC, 2013; NOAA, 2015), with increased CO_2 hydrolysis in oceanic surface water predicted to reduce the pH

* Corresponding author.
E-mail address: david.marshall@ubd.edu.bn (D.J. Marshall).

https://doi.org/10.1016/j.rsma.2017.11.004

by 0.3–0.4 by 2100 (Caldeira and Wickett, 2003; Kimmerer and Weaver, 2013). By lowering calcite and aragonite (CO_3^{2-}) saturation states, ocean acidification places calcifying organisms and ecological assemblages at greater risk (Orr et al., 2005; Kimmerer and Weaver, 2013). Contrasting with oceanic systems, estuarine CO_2 levels are mainly saturated to super-saturated, leading to net atmospheric CO_2 transfer (estuaries are generally sources of atmospheric CO_2; Borges and Gypens; Maher et al., 2015; Sadat-Noori et al., 2016). However, the carbonate chemistry of coastal systems where estuaries and oceans interact is spatially and temporally complex (Cai and Wang, 1998; Cai et al., 2011; Sunda and Cai, 2012; Call et al., 2015; Zhai et al., 2015).

Traditionally, estuarine studies focused on specific physical and chemical attributes of the water (salinity, temperature, dissolved oxygen and nutrients), with carbonate chemistry receiving limited consideration (but see Borges, 2005; Chen et al., 2012; Call et al., 2015). More recently, studies describing estuarine carbonate systems are geographically-skewed towards temperate and subtropical regions (see Laruelle et al., 2010; Noriega and Araujo, 2014; Maher et al., 2013; Maher et al., 2015) , with limited information available for tropical estuaries, especially in Southeast Asia (Koné and Borges, 2008). These estuaries are often associated with turbid river systems, productive terrestrial systems (back swamps and mangroves) and densely-populated urban areas, implying substantial nutrient (organic) loading. Excessive organic matter drives heterotrophy and aerobic respiration of resident benthic and pelagic organisms (Anderson et al., 2002; Wang, 2006; Bianchi and Allison, 2009; Cai et al., 2011; Howarth et al., 2011), which raises *in situ* water pCO_2. Additionally, pCO_2 in mangrove-dominated estuaries can be elevated by tidal pumping and within estuarine ground/porewater discharge (Borges et al., 2003; Bouillon et al., 2007; Maher et al., 2013). Furthermore, estuarine pCO_2 is affected by CO_2 importation (heterotrophy elsewhere in rivers and/or groundwater), CO_2 loss to the atmosphere (relating to wind speed and current flow; Borges et al., 2003; Zhai et al., 2005; Bouillon et al., 2007; Call et al., 2015) and exportation (relating to tidal flux and mixing; Rivkin and Legendre, 2001; Cai, 2011). Salinity robustly influences estuarine pCO_2, which is reduced at the higher salinities where an estuary enters the coastal ocean (close to equilibrium with atmospheric CO_2; Frankignoulle et al., 1998; Sarma et al., 2001; Sarma et al., 2011; Chen et al., 2012; Noriega and Araujo, 2014).

pCO_2 elevation lowers estuarine water pH (Eq. (1); Raymond et al., 2000). Nonetheless, estuarine acidification can arise through multiple other processes, including natural mineral acidic discharge (see Marshall et al., 2008). Such discharge derives from pyrite (FeS_2 in soils/sediments), which is formed under reducing conditions when marine sediments are inundated (see Acid Sulphate Soils, ASS; Dent, 1986; Powell and Martens, 2005; Grealish et al., 2008). When fossilized sediments that have been subject to sea-level-decline are disturbed by flooding or air-exposure, oxidation of the pyrite produces sulphuric acid (Fig. 1; Eq. (2); Stumm and Morgan, 1981; Dent, 1986; Schippers and Jorgensen, 2002).

$$CO_2 + H_2O \rightleftharpoons H_2CO_3 \rightleftharpoons HCO_3^- + H^+ \quad (1)$$

$$FeS_2 + 15/4O_2 + 7/2H_2O \rightarrow Fe(OH)_3 + 2H_2SO_4 \quad \text{Van Breemen (1973)} \quad (2)$$

Many coastal systems across the globe (floodplains, wetlands and estuarine embayments) are influenced by acidic groundwater infiltration (Walker, 1972; Sammut et al., 1996; Roach, 1997; Astrom and Bjorkland, 1995). Studies on the ecological consequences of ASS discharge have prominently been conducted in Australia

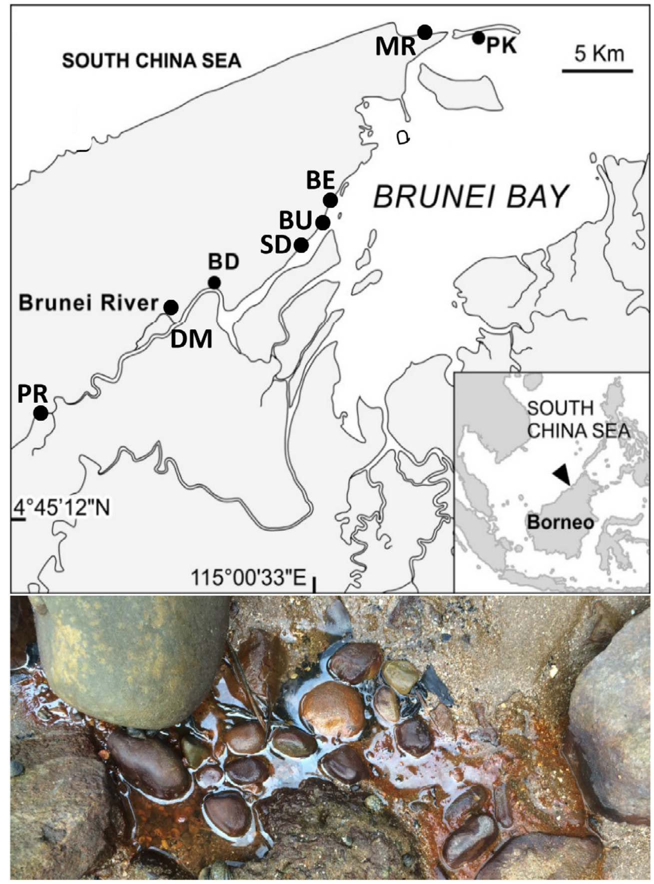

Fig. 1. Map of the Brunei Estuary System (BES) (upper panel). Sampling was carried out during Sep 2013–Mar 2014. Hydrological monitoring stations were Bandar (BD), Serdang (SD) and Pulau Pelumpong (PK). Discrete sampling for the carbonate system analysis was carried out at Kampong Parit (PR), Damuan (DM), Bandar (BD), Sungai Bunga (BU), Sungai Besar (BE), and Muara (MR). Lower panel shows a seep from pyrite-rich sediments at a nearby coastal locality, producing brown-staining precipitates of iron oxyhydroysulphate on pebbles and in the sediment (see Grealish et al., 2008). Oil-like bacterial films are associated with the seep.

(Brown et al., 1983; Callinan et al., 1993; Neal, 1993; Dove, 2003). More recent studies, also emanating from Australia, have explored the interaction of this discharge and the carbonate chemistry of estuaries (Maher et al., 2013; Ruiz-Halpern et al., 2015; Sadat-Noori et al., 2016; Jeffrey et al., 2016). Other cases might involve ASS, but this has not been explicitly indicated (see Chen and Borges, 2009; Laruelle et al., 2010; Chen et al., 2012; Noriega and Araujo, 2014; Call et al., 2015).

We investigated an ASS-influenced tropical mangrove estuary, the Brunei Estuarine System (BES) [Brunei Darussalam (Borneo), Southeast Asia; Grealish et al., 2008]. Other than representing a useful scientific model system, the BES is ecologically sensitive and socio-economically important to the country. It supports housing (an extensive water village, Kampong Ayer), artisanal fisheries, small-scale aquaculture, and several other ecosystem services, including acting as a significant nursery ground for many fish species. The circumstances of multiple source acidification (see Marshall et al., 2008) have stimulated studies on responses of species and ecological assemblages to low pH waters (Hossain et al., 2014; Bolhuis et al., 2014; Majewska et al., 2016; Proum et al., 2016, 2017). Like many other tropical systems, the BES is vulnerable to extreme weather patterns (flooding and drought). Flooding is

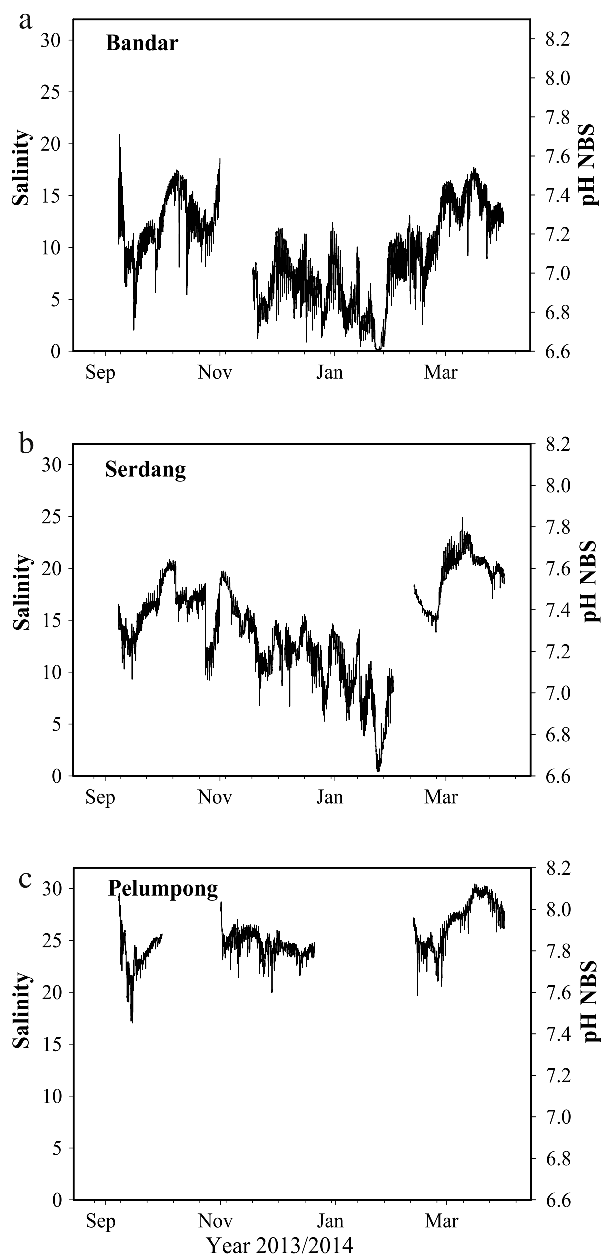

Fig. 2. Hydrological monitoring data for the BES. (a, b, and c) Salinity data were recorded every 30 min at BD, SD and PK, respectively. pH data for the same stations were derived from salinity data (see Fig. 3).

suggested to dramatically change the physical and chemical nature of the BES water (Marshall et al., 2008).

Here we describe the carbonate chemistry of an ASS-influenced tropical estuarine system (see also Koné and Borges, 2008; Ruiz-Halpern et al., 2015; Jeffrey et al., 2016). We report data that integrates the carbonate chemistry and hydrology of the BES. Specifically, we assess the spatial and temporal variations in salinity and pH and attempt to correlate these parameters with seasonal patterns of rainfall and tidal forcing. We also determine how the carbonate system parameters [surface water pH, salinity, temperature, total alkalinity (TA), pCO_2, calcite saturation (Ω_{cal}) and aragonite saturation (Ω_{ara})] vary along the BES, and how they are correlated with salinity. Finally, we explore the question of the influence of ASS discharge on the carbonate chemistry parameters.

2. Materials and methods

2.1. Study area and conditions

The Brunei Estuarine System (BES) receives freshwater via four major river systems, the Brunei and Temburong rivers (in Brunei) and the Limbang and Trusan rivers (in Sarawak, Malaysia; Andrea, 2008; Fig. 1). The water is generally brown and turbid due to high suspended sediment and organic matter loading (1–1.2 m Secchi disc depths), and is mixed vertically, with limited stratification in the upper 2–5 m of the upper estuary (Hooi, 1987; Hossain et al., 2014; Bolhuis et al., 2014). Main channel water depth varies between 2 and 12 m (with deeper holes of 26 m, Hooi, 1987). Tidal seawater influx, generated in the South China Sea (SCS), comprises mainly a semidiurnal component having a tidal range of 0–2.8 m (Hooi, 1987; Chua et al., 1987). The catchment area of the Sungai Brunei (upper and mid estuarine system considered here) is 360 km^2 (Hooi, 1987). The BES weather constitutes two general wind transitional periods, December through March (northeast monsoon) and June through October (southwest monsoon; Cooper, 1992). Intensity and times of monsoons however vary greatly within an El Niño-Southern Oscillation (ENSO) timeframe. Average rainfall varies from ∼2500 mm to > 4300 mm (Andrea, 2008).

The BES is surrounded by pristine and extensive mangrove forests. Urban development occurs mainly along the Bandar–Muara border (north-west), becoming significant towards Bandar; the confluence of Sungai Kedayang and Sungai Kianggeh at Bandar feed from distinct urban areas in the region (see Proum et al., 2016; Marshall et al., 2016; Fig. 1). The BES mudflats and surrounding terraces constitute ancient pyritic-sediments, dating to more than 5400 years ago (Bolhuis et al., 2014). These sediments are implicated in acidification of the BES, along with heterotrophic elevation of pCO_2. The natural and anthropogenic nutrification driving the latter, stems from nearby urban areas, water villages, and the extensive fringing mangroves, peat swamps and tropical forests (see Hooi, 1987). pH and salinity in the BES surface water (between Bandar and Muara) is known to range between 5.8 and 8.3 pH, and 3.58 and 31.2, respectively (see Marshall et al., 2008). In the present study, eight sampling stations were established along a 40-km stretch from the upper estuarine station of Kampong Parit (PR), in the Brunei River, to Pulau Pelumpong (PK), at the edge of the inner Brunei Bay, opposite Muara (MR) and adjacent to the SCS (Fig. 1).

2.2. Hydrological monitoring (salinity, pH, temperature and rainfall)

Conductivity and temperature loggers (HOBO U24, Onset Computer Corp., Bourne, MA, USA) were deployed at the following stations: in the upper estuary, Bandar (BD, 4°53'4.76"E, 114°56'40.27"N), the mid estuary, Serdang (SD, 4°54' 18.24"E, 115°0' 29.28"N), and the lower estuary, Pelumpong (PK, 5°2'14.57"E, 115°6' 17.56"N) (see Fig. 1). At each station, a PVC tube (of diameter 5 cm and containing 5–6 holes) was secured to a wooden pillar on a floating platform, and the logger was lowered down the tube with a nylon cord. Loggers were lowered to a depth that ensured they remained underwater at all times, and could easily be retrieved with the nylon cord to upload the data. Conductivity and temperature were recorded every 30 min, and the data were uploaded every fortnight between September 2013 and April 2014, using HOBOware software. The Practical Salinity Scale 1978 (PSS-78) was used to calculate salinity from conductivity. Epifaunal growth on the sensors was difficult to prevent, resulting in incomplete data sets in some cases.

A single pH logger (pH accuracy < 0.005; WTW WQL pH, Xylem Inc., Germany) was rotated among the different stations weekly, during Sept and Nov 2013. This was set up in the field in a similar

Table 1
Monthly mean (and range) for hydrological characteristics along the BES (Sept 2013 to March 2014). Salinity data were logged every 30 min, and pH was derived from salinity data (Fig. 3).

Parameter	Station	September	October	November	December	January	February	March
		2013				2014		
Salinity	BD	10.6 (2.1–20.8)	13.8 (5.5–18.6)	5.7 (1.2–11.5)	6.8 (1.0–12.4)	4.2 (0.1–11.3)	9.9 (2.8–16.0)	14.5 (9.0–17.7)
	SD	14.9 (9.3–19.8)	16.7 (9.3–20.8)	14.4 (6.8–19.7)	11.8 (5.3–11.8)	7.6 (0.4–14.0)	16.8 (13.8–21.7)	20.8 (17.2–24.9)
	PK	23.7 (17.0–29.5)	24.5 (17.0–28.0)	24.9 (20.0–28.7)	24.0 (21.7–25.9)	–	24.4 (20.0–27.2)	28.2 (25.1–30.4)
pH (units)	BD	6.9 (6.7–7.4)	7.1 (6.8–7.3)	6.8 (6.7–7.0)	6.8 (6.7–7.0)	6.8 (6.7 –7.0)	6.9 (6.7 –7.2)	7.1 (6.9–7.3)
	SD	7.1 (6.9–7.4)	7.2 (6.9–7.4)	7.1 (6.8–7.4)	7.0 (6.8–7.1)	6.9 (6.7–7.1)	7.2 (7.1–7.5)	7.4 (7.2–7.7)
	PK	7.6 (7.2–8.0)	7.7 (7.2–7.9)	7.7 (7.4–8.0)	7.6 (7.5–7.8)	–	7.7 (7.4–7.9)	7.9 (7.7–8.1)
Temperature (°C)	BD	29.8 (26.7–31.7)	30.2 (27.2–31.8)	29.5 (26.7–31.2)	29.6 (26.5–31.8)	27.5 (24.8–30.6)	28.9 (26.4–30.9)	30.6 (28.2–32.0)
	SD	30.5 (28.7–33.2)	30.5 (28.7–32.7)	30.8 (28.4–32.9)	30.6 (28.9–33.4)	28.5 (25.1-32.3)	29.5 (27.4–32.2)	30.7 (28.7–32.8)
	PK	30.2 (28.4–31.8)	30.1 (27.9–32.6)	30.5 (28.1–32.5)	30.8 (29.42–32.56)	–	28.9 (27.6–31.4)	29.1 (27.5–31.7)

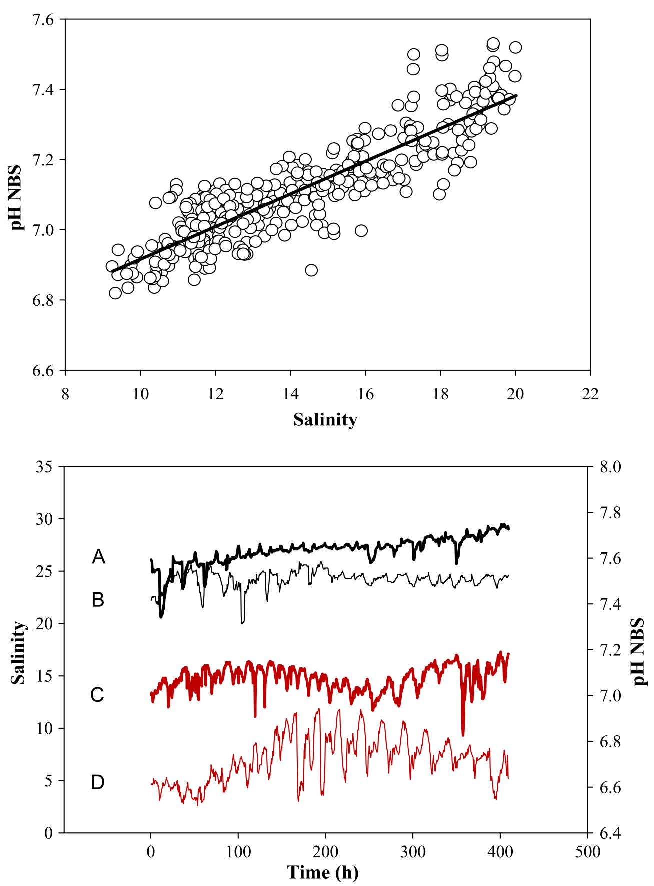

Fig. 3. Relationship between pH and salinity based on simultaneous logged data for each parameter at BD (24 Nov–11 Dec 2013, 17 days; upper panel). A linear regression (pH $= 6.45 + 0.04$ Sal, $r = 0.88$, $p < 0.001$) was used to convert salinity to pH from salinity data recorded at the other stations (Fig. 2 and below). Lower panel gives logged salinity and pH (derived) data, showing the effect of station and season. A, PK-intermonsoon (26 Feb–15 Mar); B, PK-monsoon (24 Nov–11 Dec); C, BD-intermonsoon; and D, BD-monsoon.

way to the conductivity meter (to log pH at 30-min intervals), enabling near-simultaneous recordings of pH and salinity. The logger was calibrated using a three-point US National Bureau of Standards buffer (NBS, pH = 4, 7 and 9.2) and WQL-Log software. Because reliable pH data were only attained for Bandar between 24 Oct and 2 Nov 2013, these data were used to calculate the pH for the other stations and times, using a linearly-regressed pH–salinity model.

Incidence and intensity of local rainfall were related to salinity and pH. Daily precipitation recordings were made at the Brunei International Airport (Sept–Dec 2013; courtesy of the Meteorological Department, Ministry of Communications). The effect of rainfall on pH and salinity was assessed from least-squares linear regressions for daily rainfall and daily means for pH and salinity (hydrological data set). A timescale effect (lag) was considered by averaging daily rainfall, pH and salinity, over one week, two weeks or one month, before fitting regressions. Tidal forcing was judged from pH/salinity versus tidal height (TideComp® Worldwide software; pangolin.co.nz, New Zealand; data for Dato Gandi, near Bandar) and logged salinity and pH always fell within 20 min of the tide datum used.

2.3. Surface water carbonate chemistry

2.3.1. Water sampling

Surface water was discretely sampled at six stations: in the upper estuary at Parit (PR, 4°48'20.3472"E, 114°49'57.4536"N), Dumuan (DM, 4°52'5.451"E, 114°54'37.9902"N) and Bandar (BD, 4°53'11.2272"E, 114°56'42.4638"N), middle estuary at Sungai Bunga (BU, 4°54'57.7686"E; 114°56'42.4638"N) and Sungai Besar (BE, 4°55'39.0684"E; 115°0'53.4738"N), and the lower estuary at Muara (MR, 5°2' 18.9924"E, 115°4' 48.993"N) (Fig. 1). Samples were collected from each station on five occasions. Collections were made in the morning during high tide with no rain the day before, on three occasions, between May and June 2013, and on two other occasions, between Aug and Sept 2013, after heavy rain the previous night. Station PR was an exception, with water samples taken on only four occasions during high tide after rainy days. During each sampling session, three replicates were obtained from randomly-selected areas at a given station (within 50 m of each other). The samples were collected about 0.5 m below the water surface in 500-mL white polyethylene bottles with airtight caps. The samples were poisoned with mercuric chloride (0.1–0.2 ml, Hg_2Cl_2, 50%) to avoid biological alteration (Hall-Spencer et al., 2008). The head space was eliminated in the bottles to prevent degassing of the water (Gattuso et al., 2010). Sample bottles were stored in an icebox, transferred to the laboratory within 3 h of sampling, and kept in a refrigerator at 4 °C until further analysis.

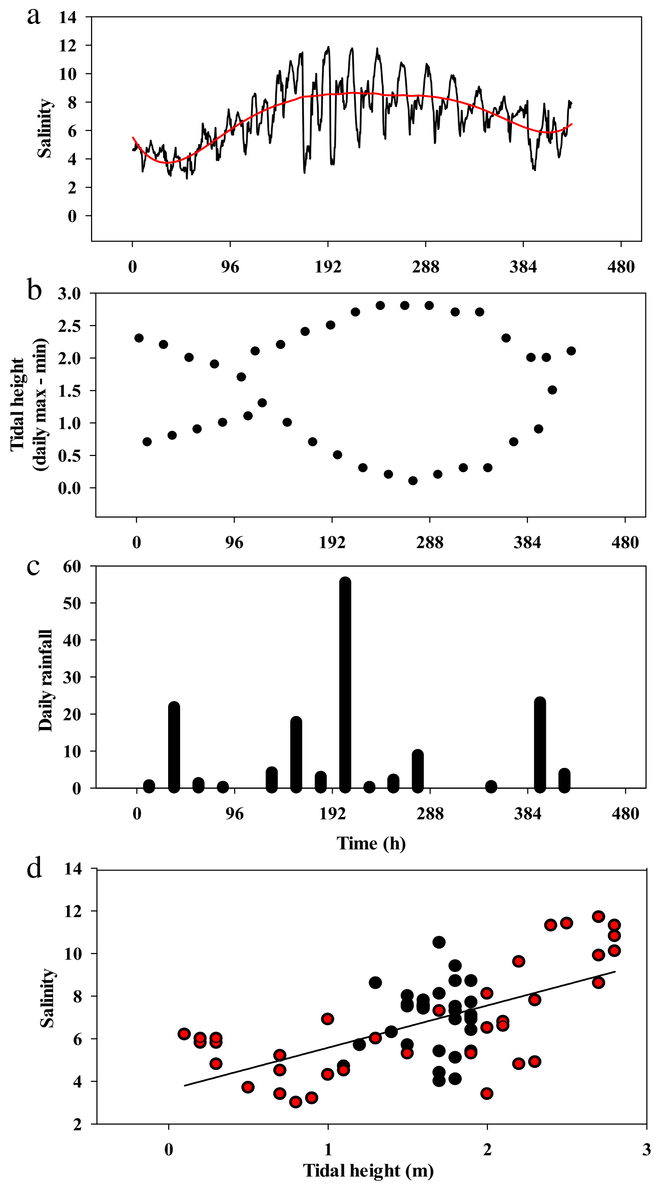

Fig. 4. Interaction between salinity, tidal height and rainfall. (a) Continuously-logged salinity at BD (24 Nov–11 Dec; Loess-smoothed curve is fitted). (b) Tidal height (maximum and minimum) near BD for the same period as in (a) above, showing spring tide at around 11 d. (c) Daily rainfall over the same period [does not change pattern of salinity in (a)]. (d) Salinity plotted against tidal height (Sal $= 3.6+ 1.9$ Tidal height, $r = 0.61, p < 0.001$); salinity is shown for daily max and min tidal heights (red symbols), as well as the harmonics for semi-diurnal tidal fluctuations (black symbols).

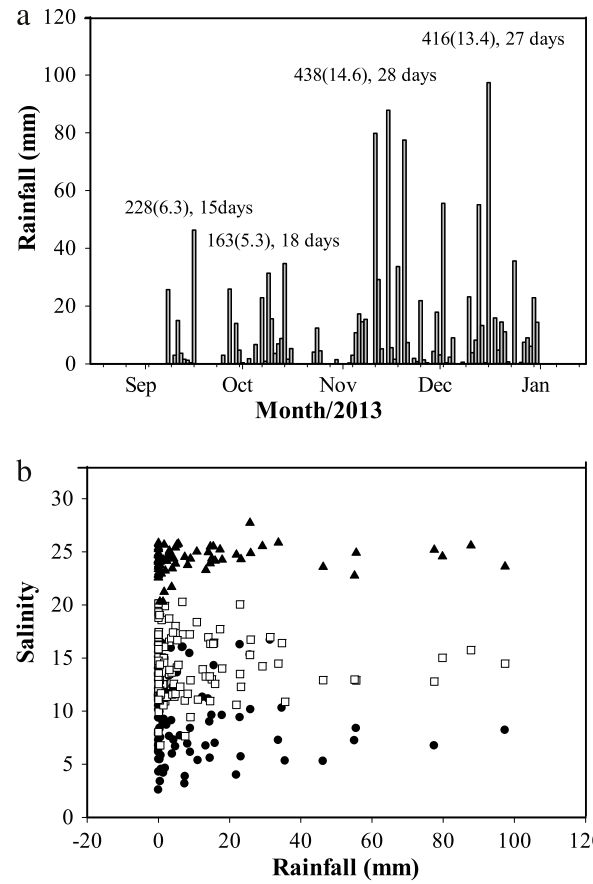

Fig. 5. Relationship between regional rainfall and salinity in the BES (Sep–Dec 2013). (a) Daily rainfall (vertical bars); values above bars are total monthly rainfall, daily mean rainfall (in parenthesis), and number of rainy days. (b) Plot for salinity against rainfall in the BES surface water. Bandar (BD, solid circles), Serdang (SD, open squares), Pulau Pelumpong (PK, solid triangles). Regression lines are not shown as they were not significant in all cases (see Table 2).

The physicochemical parameters (pH, salinity, and temperature) of the water were measured for each replicate field sample during each collection time using a pH/conductivity meter (HQ40d, HACH, Loveland, CO, USA) with two sensors attached, one for conductivity (IntelliCAL CDC401 Conductivity) and the other for pH/temperature (IntelliCAL PHC101). The pH sensor was accurate 0.01 pH units, and was freshly calibrated to three points using NBS buffers (4, 7, and 9.2) before each sampling session. The Practical Salinity Scale 1978 (PSS-78) was assumed for the meter's conversion from conductivity to salinity.

2.3.2. Carbonate system analysis

To determine the carbonate parameters, pCO_2, DIC, Ω_{cal} and Ω_{ara}, we measured TA, pH and salinity and temperature in water samples. TA in the samples was measured within 24 h of collection, following Dickson et al. (2007) (see also ISO 22719, 2008, using an indirect method, SOP 3b, open cell titration). Three replicates were used for each preserved sample titrated with HCl (0.1 N), using an automatic potentiometric titrator (G20 Compact, Mettler-Toledo International Inc., Switzerland) until an equivalent point around pH = 3 was reached. The titration system was built using a pH meter with a glass pH electrode (DGi 115-SC), initially calibrated with the three-point NBS buffer (4, 7 and 9.2), reading to an accuracy of 0.001 pH units. A 1-mL automatic burette was used to analyse an 80-mL sample at 25 °C. The pH was quantified in 0.02-mL increments of 0.1 N HCl. Values of TA in μmol kg^{-1} were calculated from a titration curve of a linear Grant function plot (Grant, 1952), using volumes of HCl (0.1 N) added to determine the equivalent point of carbonate and bicarbonate over the pH values, which varied from 3 to 4.5. Method accuracy was assessed by determining TA values of the Certificate of Reference Material (CRM) for oceanic CO_2 measurements of batch number 127 (bottled on 18 January 2013, obtained from Scripps Institute of Oceanography, USA, Dickson et al., 2003). Percentage recoveries of 97%–114% were attained, validating the method of analysis. The carbonate system parameters were calculated from measured values of pH, temperature, salinity and TA, using the CO2SYS program [with selected CO_2 constants of Millero (2010) and the NBS pH scale; written by Lewis and Wallace (1998)].

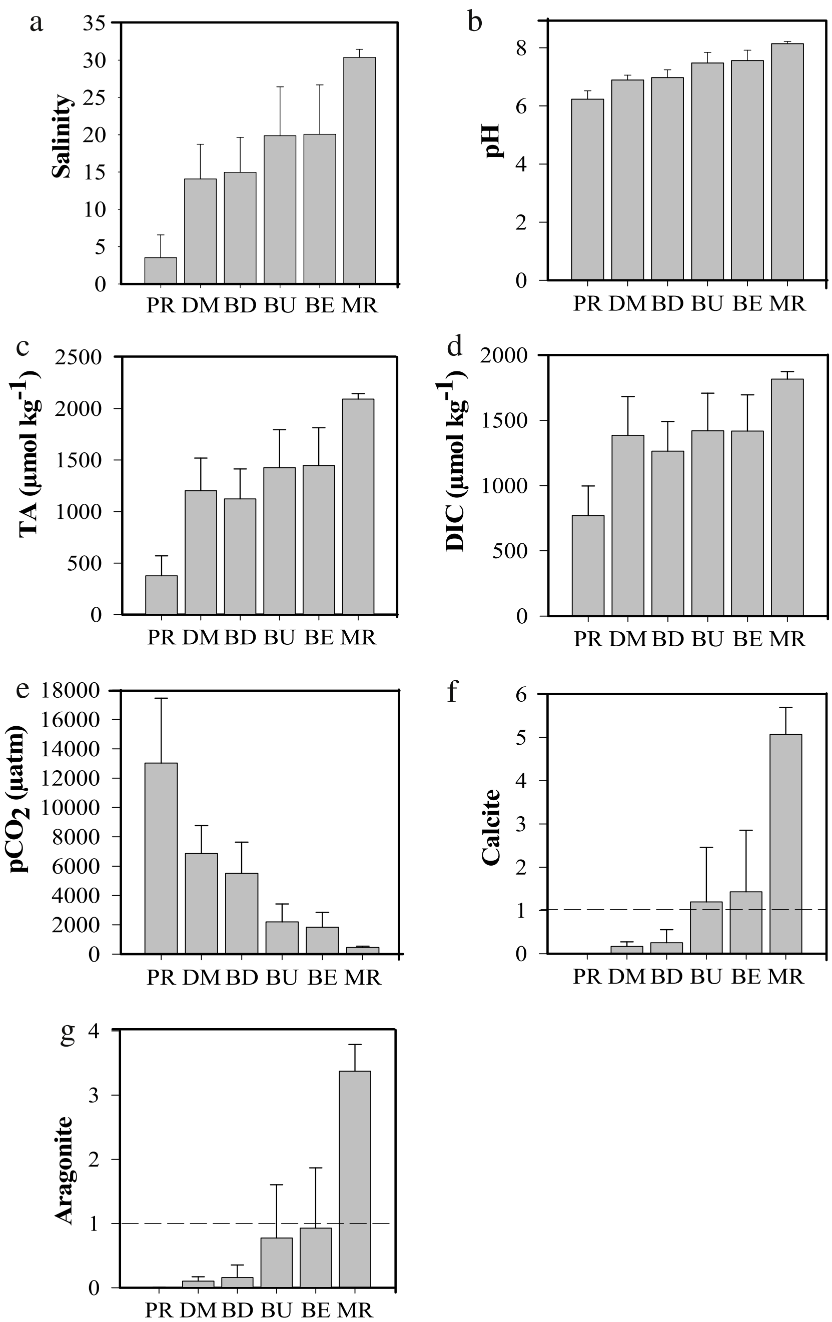

Fig. 6. Means of carbonate chemistry parameters (error bars indicate 1SD) for five sampling sessions at the six discrete sampling stations in the upper BES (PR, DM, BD), mid estuary (BU, BE), and lower estuary (MR). Horizontal lines indicate saturation level.

2.4. Statistical approach

Differences in carbonate chemistry parameters among stations were tested using nonparametric Kruskal–Wallis tests (multiple dependent variables, one factor), as the data did not pass normality tests, even after transformation. Polynomials (first or second order) were fitted to plots for salinity against carbonate system parameters. Fitted lines allowed interpolation of data; lines were meant for visual purposes and are not mechanistic predictions. All statistics and graphs were generated in either Statistica ver. 10 (Statsoft Inc., Tulsa, OK, USA) or SigmaPlot ver. 11 (Systat Software, San Jose, CA, USA).

3. Results

3.1. Hydrological dynamics (logged salinity and pH, and rainfall)

Mean monthly salinity varied greatly along the length of the estuary between 4.2 (BD, Jan) to 28.2 (PK, March; Table 1; Fig. 2). pH and salinity recordings collected simultaneously at BD correlated well (pH $=$ 6.45$+$ 0.04 Sal, $r = 0.88$; $p < 0.001$; Fig. 3), enabling conversion of logged salinity to pH for all stations (Fig. 2). Mean monthly pH (derived from the salinity relationship in Fig. 3) were BD = 6.8–7.1, SD = 6.9–7.4 and PK = 7.6–7.9 (Table 1; Fig. 2). Temperatures were relatively stable, with the monthly

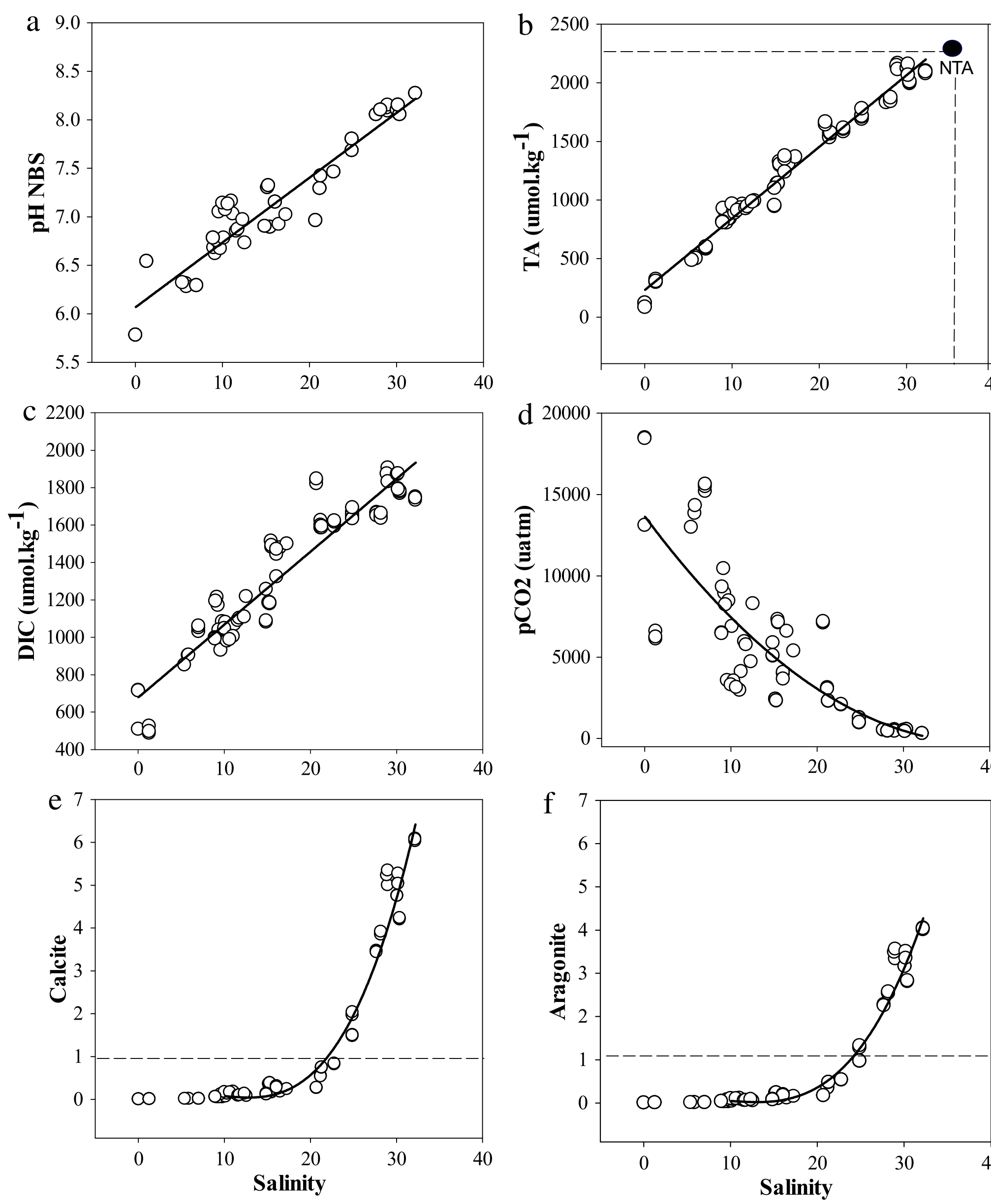

Fig. 7. Correlations between salinity and carbonate parameters for the BES surface water. Best fit lines are shown (first, second or third order polynomials). Dashed lines (b) represent the relationship between TA and salinity for the South China Sea (Bai et al., 2015; NTA) and (e and f) saturation levels. Relationships are: (a) pH = 6.07+ 0.07 Sal; (b) TA = 230.9+ 61.15 Sal; (c) DIC = 677.65+ 39.01 Sal; (d) pCO_2 = 13667.73−713.08 Sal + 9.11 Sal^2, r = 0.82; (e) Cal = 0.09+ 0.11 Sal−0.02 Sal^2 + 0.001 Sal^3; (f) Ara = 0.06+ 0.08 Sal−0.01 Sal^2 + 0.0004 Sal^3. Except where shown $0.94 < r < 0.99$, and $p < 0.001$.

mean varying between 28.9 and 30.8 °C (Table 1), though lower temperatures (below 28 °C) were recorded at BD and SD in January.

The pattern of greater variation in salinity/pH in the upper compared to the lower estuary was consistent for two timeframes, tidal and seasonal (Fig. 3). Baseline levels of these parameters were lower during monsoon compared to intermonsoon seasons, with greater parameters lowering at BD compared to PK (Figs. 2 and 3). The cyclical amplitude for pH and salinity within a tidal timeframe also increased landwards (BD; Figs. 3 and 4a), and was greater during spring tides compared to neap tides (Fig. 4a, b). Despite the different tidal phase effects, salinity correlated well with tidal height at BD (r = 0.61, $p < 0.001$, Fig. 4d). Heavy daily downpours showed little effect on daily tides during spring-tide forcing (Fig. 4a, b, c), though a seasonally cumulative effect of rainfall on salinity was evident (Figs. 2 and 5).

Monthly total precipitation from Sept through Dec 2013 at the Brunei International Airport (regional rainfall) varied between 163 and 438 mm (Fig. 5a). The wettest months were November (438 mm) and December (416 mm); these also had the most rainy days (28 and 27, respectively). Minimum rainfall and fewest rainy days occurred in Sept and Oct, with 228 and 163 mm, and 15 and 18 d, respectively. The daily precipitation maxima in Nov and Dec were 87.8 and 97.4 mm, respectively; in Sept and Oct, these values were 49.9 and 34.4 mm, respectively (Fig. 5). Daily estuarine salinity was poorly correlated with daily rainfall ($p > 0.05$; Fig. 5b; Stable 1). However, coarser timescales produced significant negative relationships at BD ($p < 0.05$); regression coefficients (r) for biweekly and monthly salinity data were 0.77 and 0.96, respectively (Table 2), outcomes consistent with a cumulative season rainfall effect.

3.2. Surface water carbonate chemistry (discrete samples)

Mean salinity increased from 3.5 at PR (upper estuary) to 30.3 at MR (lower estuary) (Fig. 6) and mean pH for these localities

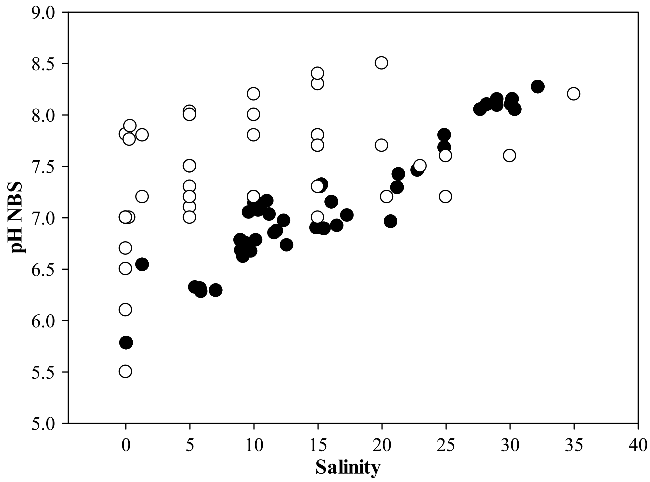

Fig. 8. pH relative to salinity for BES (closed circles; $n = 86$) compared to other estuaries in the region (open circles; $n = 40$). The BES pH–salinity relationship is shifted downwards, compared to other data, especially below salinity 20 (Bouillon et al., 2003; Cai and Wang, 1998; Chew and Chong, 2011; Koné and Borges, 2008; Martin et al., 2008; Prabu et al., 2008; Sarma et al., 2001, 2011; Zhai et al., 2007, 2015).

varied from 6.2 to 8.1, respectively. Similarly, mean TA in the surface water steadily increased seawards from 376 to 2091 µmol kg^{-1}. DIC increased seawards with a mean range from 770 to 1816 µmol kg^{-1}. Calculated pCO_2 varied from 130 31 to 450 µatm. Mean values of Ω_{cal} varied between 0.01 and 5.06 and mean Ω_{ara} between 0.004 and 3.37 (Fig. 6). Notably carbonate undersaturation commences between BU and BE, where the Brunei River enters the Brunei Bay, suggesting a strong influence on this of open sea salinity. TA, pCO_2, Ω_{cal} and Ω_{ara} in the surface water differed significantly between the upper, middle and lower estuary (Kruskal–Wallis test, $p < 0.05$; Fig. 6).

3.3. Relationships between carbonate parameters and salinity

Salinity was positively correlated with pH, TA, Ω_{cal} and Ω_{ara} and negatively correlated with pCO_2 (Fig. 7). The TA for the South China Sea was 2150–2200 µmol. kg^{-1}, consistent with a NTA (normalized TA at 33.5 salinity) of 2303±5.1µmol. kg^{-1} (Bai et al., 2015; Fig. 7). Nonlinear relationships (3rd order polynomials) for salinity against Ω_{cal} and Ω_{ara} were stable (near 0) at salinities below 20. However, regression slopes sharply increased for salinities 22–35, associated with Ω_{cal} (∼1–6.5) and Ω_{ara} (∼1–4.5). Values of Ω_{cal} and Ω_{ara} equal to 1 (saturation) were observed at salinity ∼22 and 24, respectively. Salinity and pCO_2 were non-linearly related, with an average pCO_2 at zero salinity of ∼14 000 µatm and a peak pCO_2 of ∼18 500 µatm (Fig. 7).

4. Discussion

Our data show that the BES pH and salinity vary in complex ways relative to tide, location and season. In particular, these parameters exhibited lowered baselines during monsoons and displayed increasing tidal (short-term) variability at the landward locations. With respect to carbonate chemistry, pCO_2 was supersaturated, Ω_{cal} and Ω_{ara} were undersaturated, and pH relative to salinity was extraordinary lowered, over a large portion of the estuary. Extremes in pH and pCO_2 are consistent with sulphuric acid discharge (from Acid Sulphate Soils, ASS) during monsoon seasons, when precipitation and flooding increases, and with resident heterotrophic pCO_2-generation within a tidal timeframe.

4.1. Hydrological monitoring (salinity, pH, temperature and rainfall)

As anticipated, both the high-resolution logged data (recorded every 30 min) and the discretely sampled data showed a seaward increase in salinity and pH (over a 40 km stretch). Differences between these two data sets, specifically the flatter derived salinity–pH relationship is accountable to the narrow salinity range experienced at BD (Fig. 3). This relationship for the discretely-sampled data, however, was remarkably similar to that determined in an earlier study (Marshall et al., 2008). The presently recorded mean pH values for DM, BD and MR were 6.9, 7.0, and 8.1, respectively, compared to 6.8, 6.8, and 8.0 determined for the same stations in Marshall et al. (2008). Importantly, relative to salinity, pH is distinctly lowered suggesting an extraordinary acidification effect in the BES (see below; Fig. 8).

The steep salinity and pH gradients characterizing the BES relate to the effects of tidal forcing and freshwater inflow, acting at opposite ends of the estuary. The greatest differences between daily lows and highs in salinity and pH (tidal amplitude) occurred in the upper estuary (BD), whereas seaward tidal amplitudes were relatively suppressed (PK; Figs. 2 and 3). Amplitudes also varied between neap and spring tides, being 3 to 4 times greater during spring tides at BD. Heavy daily downpours that result in run-off were found to have little effect on the BES salinity/pH regimes. Seasonal variation in freshwater (groundwater) inflow, greatly lowered baseline salinity/pH levels during monsoon months (Dec–Feb) and elevated these during intermonsoon periods (Sept–Nov; April); baseline shifts were again greatest in the upper estuary (BD; Fig. 3). Lowest monthly mean salinity was observed in Jan 2014 at BD (4.2) and SD (7.6), corresponding with the greatest monthly precipitation for this month (220–977 mm) during the previous five years (2009–2013). These observations, however, represent conditions in a mid-ENSO cycle (El Niño–Southern Oscillation), and the situation can differ in El Niño years (including Jan; see Harrison, 2000).

The intensity of the rainfall may also have a significant effect on how it influences estuarine carbonate chemistry. For example, if the rainfall is extremely intense, then much of the precipitation may runoff directly into the estuary, essentially just causing a dilution effect. If it is less intense, a greater proportion may infiltrate into the soils, where is may drive groundwater discharge due to an elevated head of pressure. This groundwater will pick up a high CO_2 load, thus having a differing influence on estuarine carbonate chemistry than direct runoff. There is often a time lag associated with this high input of groundwater following rainfall, which may also explain the stronger bi-weekly correlations observed (BD, Table 2).

4.2. Carbonate parameter, pH and salinity relationships

Salinity and pH were strongly positively correlated with TA, DIC, Ω_{cal} and Ω_{ara} ($r > 0.90$), and were negatively correlated with pCO_2 ($r = -0.82$). Salinity was non-linearly related to the saturation state of calcite and aragonite. Saturation equilibria (Ω_{cal} and $\Omega_{ara} = 1$) occurred, respectively, at salinities of ∼22 and ∼24, marking where the Sungai Brunei enters the Brunei Bay (BU and BE; Fig. 1). Differences in carbonate chemistry of the waterbodies imply different ecological consequences. Calcite and aragonite ($\Omega < 1$) under-saturation in the upper estuary will limit calcification and cause increased shell dissolution of inhabitant species of barnacle, serpulid worms and molluscs (see Feely et al., 2009). Although gastropods thrive in the upper estuary (near BD), their shells are grossly eroded compared to seaward populations (Marshall et al., 2008; Marshall, 2009; Proum et al., 2017).

Compared to other regional estuaries, the BES constitutes a low pH relative to salinity; the absolute extremes in pH were 6.23

(at 3.53 salinity) and 8.14 (at salinity 30.37) (see Fig. 8). Whereas pH 7 usually associates with salinities of < 1, in the BES this pH level was recorded for salinities up to 20 (Fig. 8, and references therein). Extraordinary acidification can develop from several different sources, including (i) ASS discharge, (ii) acidic water inflow from adjacent peat swamps (acidic phytochemicals, tannins, etc.), and (iii) direct anthropogenic sources (from the densely-urbanized areas of Gadong, Kuilap and Bandar; see Marshall et al., 2008). However, predominant drivers of the BES acidification apparently relate to heterogenically-elevated pCO_2 levels (Eq. (1)) and natural acidic inflows (ASS discharge; Grealish et al., 2008; Eq. (2)). Sulphide levels were not determined, but the BES is known to carry high total S and Fe^{2+} loads; reported sediment levels for these at BD are, respectively, 13 820 and 22 720 mg kg^{-1}dw (Hooi, 1987), and gastropod tissue Fe concentrations increased consistently towards BD (between 352 and 683 μg g^{-1}dw; (Proum et al., 2016)). Distribution patterns of these element concentrations are difficult to explain other than through ASS-influence, a phenomenon widespread in Asia (Kuwantani and Nishii, 1969; Sammut et al., 1996).

4.3. pCO_2 variation in the BES

Like many estuarine systems, pCO_2 in the BES surface water is oversaturated with respect to the atmospheric CO_2equilibrium (~400 μatm; NOAA, 2015), such that the BES represents a net CO_2 source to the atmosphere (see Cloern et al., 2014). Although the pCO_2 rapidly declined seawards, as seen in other estuarine systems (Sarma et al., 2001, 2011; Chen et al., 2012; Noriega and Araujo, 2014), values calculated for the upper stream were extraordinarily high (around 33 fold atmospheric levels). Unusually high pCO_2 values in freshwater systems have been attributed to calculation error, specifically not considering non-carbonate ions in total alkalinity calculations (TA; (Hunt et al., 2011; Abril et al., 2015)). Such overestimation however applies mainly to very low TA conditions ($<$1000 μmol/kg; Abril et al., 2015), whereas the BES pCO_2 levels were relatively high (above 10,000 μatm) at a TA of 1000 μmol/kg (salinity 10; see Fig. 7). The pCO_2levels mostly exceeded those reported for other estuarine systems [New South Wales, Australia (4000–6000 μatm; Maher et al., 2015), global estuaries (3033 $\pm$1.078 μatm; Chen et al., 2012), Brazil (2674 μatm; Noriega and Araujo, 2014), Changjiang, China (642–1445 μatm; Zhai et al., 2007), and Papua New Guinea (465–2565 μatm; Borges et al., 2003)], but favourably compared with levels (26,106 μatm) determined directly (not calculated) for similar mineral-acidified subtropical systems in Australia (Call et al., 2015, see also Ruiz-Halpern et al., 2015; Jeffrey et al., 2016; Sadat-Noori et al., 2016).

Elevated pCO_2 levels are generally assumed to relate to (i) freshwater dilution of Ca^{2+} and CO_2^{3-}, (ii) rock and soil type, (iii) water–atmosphere interactions, (iv) heterotrophic microbial CO_2 generation (in benthic sediments and the water column) and (v) acidic groundwater inflow. Because estuaries receive large quantities of organic matter (including organic carbon) from land and river ecosystems (Cloern et al., 2014) they support prominent heterotrophy. Additionally, mangrove sediments are joined tidally to creeks that carry high organic carbon loads (Alongi, 2009). While the significance of mangrove-derived carbon from food webs in adjacent systems is controversial (Nagelkerken et al., 2008), rich microbial benthic communities (including that of Archaea, bacteria and fungi) capable of transforming organic matter (mangrove leaf litter) into inorganic nutrients and CO_2, characterize the BES (Bolhuis et al., 2014). Resident heterotrophy in the upper BES is further implied by characteristically low levels of dissolved oxygen (DO) and high nutrient loading (at the station BD, DO < 4 mg l^{-1}, $NO_2 > 80$ ug l^{-1} and $NO_3 > 0.3$ mg l^{-1}; Hooi, 1987).

Table 2
Effect of timeframe on the relationship between rainfall and salinity at three stations in the BES. Indices and coefficients refer to the linear regression, Salinity = $\alpha + \beta *$ Rainfall. Station symbols refer to Pulau Pelumpong (PK), Serdang (SD) and Bandar (BD). Salinity and rainfall data were averaged for days, weeks, two weeks and months. Bold indicates a significant relationship.

Timeframe	Station	α	β	r	p
Daily	PK	24.11	0.01	0.18	0.12
	SD	14.48	0.005	0.03	0.76
	BD	10.04	0.03	0.14	0.17
Weekly	PK	23.74	0.043	0.04	0.2
	SD	14.87	−0.051	0.16	0.54
	BD	11.42	−0.17	0.41	0.13
Biweekly	PK	24.04	0.017	0.12	0.82
	SD	16.73	−0.22	0.49	0.22
	BD	14.25	−0.48	0.77	**0.04**
Monthly	PK	23.88	−0.044	0.39	0.61
	SD	17.55	−0.32	0.74	0.26
	BD	16.58	−0.77	0.96	**0.04**

Sulphuric acidic discharge can potentially raise pCO_2 through DIC speciation and a shift in the carbonate system equilibrium, due to vast proton addition Eqs. (3) and (4). Although a study connecting the geology with estuarine CO_2 levels found no correlation between rock properties and water CO_2 (Noriega and Araujo, 2014), ASS was not specifically implicated.

$$H_2SO_4 \rightarrow HSO_4^- + H^+ \tag{3}$$

$$CO_3^{2-} + 2H^+ \rightleftharpoons HCO_3^- + H^+ \rightleftharpoons H_2CO_3 \rightleftharpoons CO_2 + H_2O \tag{4}$$

The effect of mineral acidification in raising estuarine pCO_2 is likely to be greatest during the monsoon season, when groundwater discharge into the BES is most prevalent. At times when acidic groundwater inflows are reduced, during low rainfall intermonsoon conditions, resident heterotrophy (within the estuarine system) likely contributes more prominently to tidal pCO_2 variation.

4.4. Concluding remarks

Our knowledge of the interactive effects of pCO_2 and mineral acidification in ASS-influenced estuarine systems is currently mechanistically and geographically limited. Here we describe tidal and seasonal variation in pH and salinity fluxes, when heterotrophic (pCO_2) and mineral (H_2SO_4) acidification processes are likely to be of greater or lesser significance. Importantly, our findings suggest that mineral acidification is likely to elevate pCO_2 to extraordinarily high levels. Because shifts in carbonate chemistry carry significant ecological structural and functional consequences, this topic deserves more detailed future consideration.

Acknowledgements

This study was funded through a Brunei Research Council grant (UBD/GRS/S&T/16). Sorya Proum received Ph.D. support from this grant, as well as from the International Science Program (ISP) of Uppsala University, Sweden, and the Royal University of Phnom Penh (RUPP), Cambodia (IPICS CAB:1). The authors thank Jason Hall-Spencer, Andrew Dickson, Belal Hossain for suggestions on the experimental design, calculation of the carbonate parameters, and useful discussions. We also thank A. Musim for setting up the field data recording instruments and Vanessa Teo for the providing rainfall data. The manuscript was much improved by the inclusion of comments of two reviewers.

References

Abril, G., Bouillon, S., Darchambeau, F., Teodoru, C.R., Marwick, T.R., Tamooh, F., Omengo, F.O., Geeraert, N., Deirmendjian, L., Polsenaere, P., Borges, A.V., 2015. Technical Note: large overestimation of pCO2 calculated from pH and alkalinity in acidic organic-rich fresh waters. Biogeosciences 12, 67–78.

Alongi, D.M., 2009. Energetics of Mangroves. Springer Science, Business Media B.V., New York, USA, ISBN: 978-1402042706.

Anderson, D.M., Glibert, P.M., Burkholder, J.M., 2002. Harmful algal blooms and eutrophication: Nutrient sources, composition and consequences. Estuar. 25 (4b), 704–726.

Andrea, B., 2008. Asian water bird census, Brunei Darussalam. Method description 2008 census results. AWC.2008. Brunei Darussalam.

Astrom, M., Bjorkland, A., 1995. Impact of acid sulfate soils on stream water geochemistry in western Finland. J. Geochem. Explor. 55, 163–170.

Bai, Y., Huang, T.-H., He, X., Wang, S.-L., Hsin, Y.C., Wu, C.-R., Zhai, W., Lui, H.-K., Chen, C-T.A., 2015. Intrusion of the Pearl River plume into the main channel of the Taiwan Strait in summer. J. Sea Res. 95, 1–15.

Bianchi, T.S., Allison, M.A., 2009. Large-river delta-front estuaries as natural "recorders" of global environmental change. Proc. Natl. Acad. Sci. USA 106, 8085–8092.

Bolhuis, H., Schluepmann, H., Kristalijn, J., Sulaiman, Z., Marshall, D.J., 2014. Molecular analysis of bacteria diversity in mudflats along the salinity gradient of acidified tropical Bornean estuary (South East Asia). Aquat. Biosyst. 10, 10.

Borges, A.V., 2005. Do we have enough pieces of the jigsaw to integrate CO_2 fluxes in coastal ocean? Estuar. 28 (1), 3–27.

Borges, A.V., Djenidi, S., Lacroix, G., Theate, J., Delille, B., Frankignoulle, M., 2003. Atmospheric CO_2flux from mangrove surrounding waters. Geophys. Res. Lett. 30 (11). http://dx.doi.org/10.1029/2003gl017143.

Borges, V.A., Gypens, N., 2010. Carbonate chemistry in the coastal zone responds more strongly to eutrophication than to ocean acidification. Limnol. Oceanogr. 55 (1), 346–353.

Bouillon, S., Frankignoulle, M., Dehairs, F., Velimirov, B., Eiler, A., Abril, G., Etcheber, H., Borges, A.V., 2003. Inorganic and organic carbon biogeochemistry in the Gautami Godavari estuary (Andhra Pradesh, India) during pre-monsoon: the local impact of extensive mangrove forests. Glob. Biogeochem. Cy. 17, 1114. http://dx.doi.org/10.1029/2002gb002026.

Bouillon, S., Middelburg, J.J., Dehairs, F., Borges, A.V., Abril, G., 2007. Importance of intertidal sediment processes and porewater exchange on the water column biogeochemistry in a pristine mangrove creek (Ras Dege, Tanzania). Biogeosciences 4 (3), 311–322.

Brown, T.E., Morley, A.W., Sanderson, N.T., Tait, R.D., 1983. Report of a large fish kill resulting from natural acid water conditions in Australia. J. Fish Biol. 22, 335–350.

Cai, W.J., 2011. Estuarine and coastal ocean carbon paradox: CO_2 sinks or sites of terrestrial carbon incineration? Ann. Rev. Mar. Sci. 3, 123–145.

Cai, W.J., Hu, X., Huang, J.W., Murrell, M.C., Lehrter, J.C., Lohrenz, S.E., Chou, W.C., Zhai, W., Hollibaugh, J.T., Wang, Y., Zhao, P., Guo, X., Gundersen, K., Dai, M., Gong, G.C., 2011. Acidification of subsurface coastal waters enhanced by eutrophication. Nat. Geosci. Lett. 23, 20.1038/NGEO1297.

Cai, W.J., Wang, Y., 1998. The chemistry, fluxes, and sources of carbon dioxide in the estuaries water of the Satilla and Atamaha rivers Georgia. Limnol. Oceanogr. 43 (4), 657–668.

Caldeira, K., Wickett, M.E., 2003. Anthropogenic carbon and ocean pH. Nat. Brief Commun. 425, 356.

Call, M., Maher, D.T., Santos, I.R., Ruiz-Halpern, S., Mangion, P., Sanders, C.J., Erler, D., Oakes, V., Rosentreter, J., Muarray, R., Eyre, B.D., 2015. Spatial and temporal variability of carbon dioxide and methane fluxes over semi-diurnal and spring-neap-spring timescales in a mangrove creek. Geochim. Cosmochim. Acta. 150, 211–225.

Callinan, R.B., Fraser, G.C., Melville, M.D., 1993. Seasonally recurrent fish mortalities and ulcerative disease outbreaks associated with acid sulphate soils in Australian estuaries. In Dent, D., and van Mensvoort, M. E. F. (Eds.) Selected Papers of the Ho Chi Minh City Symposium on acid sulphate soils, ILRI Publication No. 53, International Institute for Land Reclamation and Improvement, Wageningen, The Netherlands, pp. 403–410.

Chen, C.T.A., Borges, A.V., 2009. Reconciling opposing views on carbon cycling in the coastal ocean: continental shelves as sinks and near-shore ecosystems as sources of atmospheric CO_2. Deep- Sea Res. II-Top. Stud. Oceanogr. 56, 578–590. http://dx.doi.org/10.1016/j.dsr2.2009.01.001.

Chen, C.-T.A., Huang, T.-H., Fu, Y.-H., Bai, Y., He, X., 2012. Strong sources of CO_2in upper estuaries become sinks of CO_2 in large river plumes. Curr. Opin. Environ. Sustainability 4, 179–185.

Chew, L.L., Chong, V.C., 2011. Copepod community structure and abundance in a tropical mangrove estuary, with comparisons to coastal waters. Hydrobiologia 666, 127–143. http://dx.doi.org/10.1007/s10750-010-0092-3.

Chua, T.-E., Chou, L.M., Sadorra, M.S.M., 1987. The coastal environmental profile of Brunei Darussalam: resource assessment and management issues. ICLARM Technical Report 18. Fisheries Department, Ministry of Development, Brunei Darussalam.

Cloern, J.E., Foster, S.Q., Kleekner, A.E., 2014. Phytoplankton primary production in the world's estuarine coastal ecosystems. Biogeosciences 11, 2477–2501.

Cooper, R., 1992. Forecast and understanding local weather in Brunei Darussalam. Brunei Museum J. 7 (4), 88–98.

Dent, D., 1986. Acid sulphate soils: A baseline for research and development. ILRI Publication No. 39. International institute for land Reclamation and improvement: Wageningen.

Dickson, A.G., Afghan, J.D., Anderson, G.C., 2003. Reference materials for oceanic CO_2 analysis: a method for the certification of total alkalinity. Mar. Chem. 80, 185–197.

Dickson, A.G., Sabine, C.L., Christian, J.R., 2007. Guide to best practices for ocean CO_2 measurements. Pices Special Publication 3, IOCCP REPORT No. 8.

Dove, M.C., 2003. Effect of Estuarine Acidification on Survival and Growth of the Sydney Rock Oyster Saccostrea Glomerata. School of Geography; The University of New South Wales, Sydney, (Ph.D. Thesis).

Feely, R.A., Doney, S.C., Cooley, S.R., 2009. Ocean acidification: Present conditions and future changes in a high CO_2 world. Oceanogr. 22 (4), 36–47.

Frankignoulle, M., Abril, G., Borges, A.V., Bourge, I., Canon, C., DeLille, B., Libert, E., Theate, J.M., 1998. Carbon dioxide emissions from European estuaries. Science 282, 434–436. http://dx.doi.org/10.1126/science.282.5388.434.

Gattuso, J.P., Gao, K.,, Lee.,K., Rost, B., Schulz, G.K., 2010. Approaches and tools to manipulate the carbonate chemistry. Cited in Riebessell, U., Fabry V.J., Hansson L., Gattuso J.P. (Eds). Guide to the best practices for ocean acidification researchers and data reporting. 2010, pp. 43–55. European Project on Ocean Acidification. European Commission publication, 263 pp.

Grant, G., 1952. Determination of the equivalence point in potentiometric titrations. Part II. Anal. 77, 661–671.

Grealish, G., Fitzpatrick, R., Ringrose-Voase, A., Hicks, W., 2008. Brunei: summary of acid sulfate soils, in: Fitzpatrick, R., Shand P. (Eds.), Inland acid sulfate soil systems across Australia. CRC LEME Open File Report No. 249. (Thematic Volume) CRC LEME, Perth, Australia, pp. 301–309.

Hall-Spencer, J.M., Rodolfo-Metalpa, R., Martin, S., Ransome, E., Fine, M., Turner, S.M., Rowley, S.J., Tedesco, D., Buia, M.C., 2008. Volcanic carbon dioxide vents show ecosystem effects of ocean acidification (supplementary information). Nature 454, 96–99.

Harrison, D.R., 2000. Repercussions of El Niño: drought cause extinction and the breakdown of mutualism in Borneo. Proc. R. Soc. Land. B. 267, 911–915.

Hooi, S.D.M., 1987. Sungai Brunei water quality and pollution study. Government of Negara Brunei Darussalam Jabatan Keraja Raya. Final Report. February, 1987.

Hossain, M.B., Marshall, D.J., Venkatramanan, S., 2014. Sediment granulometry and organic matter content in the intertidal zone of the Sungai Brunei Estuarine System, northwest coast of Borneo. Carpathian J. Earth. Environ. Sci. 9, 231–239.

Howarth, R., Chan, F., Conley, D.J., Camier, J., Donney, S.C., 2011. Coupled biogeochemical cycles: eutrophication and hypoxia in temperate estuaries and coastal marine ecosystems. Front. Ecol. Environ. 9, 18–26.

Hunt, C.W., Salisbury, J.E., Vandemark, D., 2011. Contribution of non-carbonate anions to river alkalinity and overestimation of pCO_2. Biogeosci. Discuss. 8, 5159–5177.

IPCC, 2013. Climate Change 2013: The Physical Science Basis. Contribution of Working Group I to the Fifth Assessment Report of the Intergovernmental Panelon Climate Change. Cambridge University Press, Cambridge, United Kingdom and New York, NY, USA.

Jeffrey, L.C., Maher, D.T., Santos, I.R., McMahon, A., Tait, D.R., 2016. Groundwater, acid and carbon dioxide dynamics along a coastal wetland, lake and estuary continuum. Estuar. Coast. http://dx.doi.org/10.1007/s12237-016-0099-8.

Kimmerer, W., Weaver, M.J. (Eds.), 2013. Vulnerability of Estuaries to Climate Change, Vol. 4. San Francisco State University, Elsevier Inc, Tiburon, CA, pp. 271–292 Climate Vulnerability.

Koné, Y.J.M., Borges, A.V., 2008. Dissolved inorganic carbon dynamics in the waters surrounding forested mangroves of the Ca Mau Province (Vietnam). Estuar. Coast. Shelf Sci. 77, 409–421.

Kuwantani, Y., Nishii, T., 1969. Effects of decreased pH of culture water on the growth of the Japanese pearl oyster. Bull. Japan. Soc. Sci. Fish. 35, 342–350.

Laruelle, G.G., Du¨rr, H.H., Slomp, C.P., Borges, A.V., 2010. Evaluation of sinks and sources of CO_2 in the global coastal ocean using spatially-explicit typology of estuaries and continental shelves. Geophys. Res. Lett. 37, L15607.

Lewis, E., Wallace, D.W.R., 1998. Program developed for CO_2 system calculation. Oak Ridge, Tennessee: ORNL/CDIAC-105. Carbon Dioxide Information Analysis Centre, Oak Ridge National Laboratory, U.S. Department of Energy.

Maher, D.T., Cowley, K., Santos, I.R., Macklin, P., Eyre, B.D., 2015. Methane and carbon dioxide dynamic in a subtropical estuary over a diel cycle: insights from automated in situ radioactive and stable isotope measurements. Mar. Chem. 168, 69–79.

Maher, D.T., Santos, I.R., Golsby-Smith, L., Gleeson, J., Eyre, B.D., 2013. Groundwater-derived dissolved inorganic and organic carbon exports from a mangrove tidal creek: The missing mangrove carbon sink? Limnol. Oceanogr. 58 (2), 475–488. http://dx.doi.org/10.4319/lo.2013.58.2.0475.

Majewska, R., Adam, A., Mohammad-Noor, N., Convey, P., De Stefano, M., Marshall, D.J., 2016. Spatio-temporal variation in phytoplankton communities along a salinity and pH gradient in a tropical estuary (Brunei, Borneo, South East Asia). Trop. Ecol. 58, 251–269.

Marshall, D.J., 2009. Predatory and reproductive responses of the estuarine whelk *Thais gradata* (Caenogastropoda: Muricidae) to novel colonization by *Musculista senhousia* (Bivalvia: Mytilidae). J. Mar. Biol. Assoc. UK 89, 1387–1393.

Marshall, D.J., Proum, S., Hossain, B., Adam, A., Lim, L.H., Santos, J.H., 2016. Ecological responses to fluctuating and extreme marine acidification: lessons from a tropical estuary (the Brunei Estuarine System). Sci. Bruneiana 15, 1–17.
Marshall, D.J., Santos, J.H., Leung, K.M.Y., Chak, W.H., 2008. Correlation between gastropod shell dissolution and water chemical properties in a tropical estuary. Mar. Environ. Res. 66, 422–429.
Martin, G.D., Vijay, J.G., Laluraj, C.M., Madhu, N.V., Joseph, T., Nair, M., Gupta, G.V.M., Balachandran, K.K., 2008. Fresh water influence on nutrient stoichiometry in a tropical estuary, southwest coast of India. Appl. Ecol. Env. Res. 6 (1), 57–64.
Millero, F.J., 2010. Carbonate constant for estuarine waters. Mar. Freshw. Res. 61, 139–142.
Nagelkerken, I., Blabe, S.J.M., Bouillon, S., Green, P., Haywood, ., Kirton, L.G., Meynecke, J.-O., Pawlik, J., Penrose, H.M., Sasekumar, A., Somerfield, ., 2008. The habitat function of mangroves for terrestrial and marine fauna. Rev. Aquat. Bot. 89, 155–185.
National Oceanic and Atmospheric Administration (NOAA), 2015. Trends in atmospheric CO_2–recent Mauna Loa CO_2. http://www.esrl.noaa.gov/gmd/ccgg/trends/ (accessed 16.06.15).
Neal, H., 1993. Integrated Project: The effects of run-off from acid sulphate soils on benthic communities –a study site at Tuckean Swamp, NSW. Centre for Coastal Management, Southern Cross University, Lismore, NSW, Australia.
Noriega, C., Araujo, M., 2014. Carbon dioxide emissions from estuaries of northern and northeastern Brazil. Natur. Sci. Rep. 4, 6164.
Orr, J.C., Fabry, V.J., Aumont, O., Bopp, L., Doney, S.C., Feely, R.A., Gnanadesikan, A., Gruber, N., Ishida, A., Joos, F., Key, R.M., Lindsay, K., Maier-Reimer, E., Matear, R., Monfray, P., Mouchet, A., Najjar, R.G., Plattner, G.K., Rodgers, K.B., Sabine, C.L., Sarmiento, J.L., Schlitzer, R., Slater, R.D., Totterdell, I.J., Weirig, M.-F., Yamanaka, Y., Yool, A., 2005. Anthropogenic ocean acidification over the twenty –first century and its impact on calcifying organisms. Nature 437, 681–686. http://dx.doi.org/10.1038/nature04095.
Powell, B., Martens, M., 2005. A review of acid sulfate soil impacts, actions and policies that impact on water quality in Great Barrier Reef catchments, including a case study on remediation at East Trinity. Mar. Pollut. Bull. 51, 149–164.
Prabu, V.A., Rajkumar, M., Perumal, P., 2008. Seasonal variations in physico-chemical parameters in Uppanar estuary, Cuddalore (southeast coast of India). J. Mar. Biol. Assoc. India 50 (2), 161–165.
Proum, S., Harley, C.D., Steele, M., Marshall, D.J., 2017. Aerobic and behavioral flexibility allow estuarine gastropods to flourish in rapidly changing and extreme pH conditions. Mar. Biol. 164, 97.
Proum, S., Santos, J.H., Lim, L.H., Marshall, D.J., 2016. Metal accumulation in the tissues and shells of *Indothais gradata* snails inhabiting soft and hard substrata in an acidified tropical estuary (Brunei, South East Asia). Reg. Stud. Mar. Sci. 8, 487–497.
Raymond, P.A., Bauer, J.E., Cole, J.J., 2000. Atmospheric CO_2 evasion, dissolved inorganic carbon production, and net heterotrophy in the York River estuary. Limnol. Oceanogr. 45 (8), 1707–1717.
Rivkin, R.B., Legendre, L., 2001. Biogenic carbon cycles in the upper ocean: effects of microbial respiration. Science 291 (5512), 2398–2400. http://dx.doi.org/10.1126/science.291.5512.2398.
Roach, A.C., 1997. The effect of acid water inflow on estuarine benthic and fish communities in the Richmond River, N.S.W. Australia. Aust. J. Ecotoxicol. 3, 25–56.
Ruiz-Halpern, S., Maher, D.T., Santos, I.R., Eyre, B.D., 2015. High CO2 evasion during floods in an Australian subtropical estuary downstream from a modified acidic floodplain wetland. Limnol. Oceanogr. 60 (1), 42–56. http://dx.doi.org/10.1002/lno.1004.
Sadat-Noori, M., Maher, D.T., Santos, I.R., 2016. Groundwater discharge as a source of dissolved carbon and greenhouse gases in a subtropical estuary. Estuar. Coast. 39 (3), 639–656. http://dx.doi.org/10.1007/s12237-015-0042-4.
Sammut, J., White, I., Melville, M.D., 1996. Acidification of an estuarine tributary in eastern Australia due to drainage of acid sulfate soils. Mar. Freshw. Res. 47, 669–684. http://dx.doi.org/10.1071/MF9960669.
Sarma, V.V.S.S., Kumar, M.D., Manerikar, M., 2001. Emission of carbon dioxide from a tropical estuarine system, Goa, India. Geophys. Res. Lett. 28 (7), 1239–1242.
Sarma, V.V.S.S., Kumar, N.A., Prasad, V.R., Venkataramana, V., Appalanaidu, S., Sridevi, B., Kumar, B.S.K., Bharati, M.D., Subbaiah, C.V., Acharaya, T., Rao, G.D., Viswanadham, R., Gawade, L., Manjary, D.T., Kumar, P.P., Rajeev, K., Reddy, N.P.C., Sarma, V.V., Kumar, M.D., Sadhuran, Y., Murty, T.V.R., 2011. High CO_2 emission from tropical Godavari estuary (India) associated with monsoon river discharges. Geophys. Res. Lett. 38, L08601 10.1029.
Schippers, A., Jorgensen, B.B., 2002. Biogeochemistry of pyrite and iron sulphide oxidation in marine sediments. Geochim. Cosmochim. Acta 66 (1), 85–92.
Stumm, W., Morgan, J.W., 1981. Aquatic Chemistry: An Introduction Emphasising Chemical Equilibria in Natural Waters, second ed. Wiley, New York.
Sunda, G.W., Cai, W.J., 2012. Eutrophication induced CO_2-acidification of surface coastal water: interactive effects of temperature, salinity and atmospheric pCO_2. Environ. Sci. Technol. 46 (1), 10651–10659.
Van Breemen, N., 1973. Soil forming processes in acid sulphate soils. In 'Acid Sulphate Soils: Proceedings of the International Symposium on Acid Sulphate Soils, 13–20 August 1972, Dost H. (Ed.). International Institute for Land Reclamation and Improvement. Wageningen, The Netherlands, pp. 66–129.
Walker, P.H., 1972. Seasonal and stratigraphic controls in the coastal floodplain soils. Aust. J. Soil Res. 10, 127–142.
Wang, B., 2006. Cultural eutrophication in the Changjiang (Yangtze River) plume: history and perspective. Estuar. Coast. Shelf Sci. 69, 471–477.
Zhai, W.D., Dai, M.H., Cai, W.-J., Wang, Y.C., Wang, Z.H., 2005. High partial pressure of CO_2 and its maintaining mechanism in a subtropical estuary: the Pearl River estuary, China. Mar. Chem. 93, 21–32.
Zhai, W., Dai, M., Guo, X., 2007. Carbonate system and CO_2 degassing fluxes in the inner estuary of Changying (Yangtze) River, China. Mar. Chem. 107, 342–356.
Zhai, W.D., Zang, K.P., Huo, C., Zheng, N., Xu, X.-M., 2015. Occurrence of aragonite corrosive water in the North Yellow Sea, near the Yalu River estuary, during a summer flood. Estuar. Coast. Shelf Sci. 166, 199–208.